

# Complete $\mathcal{O}(N_f\alpha^2)$ Weak Contributions to the Muon Lifetime

Paresh Malde and Robin G. Stuart

*Randall Physics Laboratory, University of Michigan  
Ann Arbor, MI 48109-1120, USA*

---

## Abstract

The complete  $\mathcal{O}(N_f\alpha^2)$  weak contributions to the muon lifetime, denoted as  $\Delta r^{(2)}$ , are calculated in the  $\overline{\text{MS}}$  renormalization scheme. These come from 2-loop Feynman diagrams containing a loop formed by complete generations of massless fermions. They form an independent, gauge-invariant set of corrections that, because of the large number of light fermions in the Standard Model, is expected to make a significant contribution. In the  $\overline{\text{MS}}$  renormalization scheme with  $\mu' \equiv (\pi e^\gamma)^{\frac{1}{2}} \mu = M_Z$  and for a Higgs mass,  $M_H$ , in the range 100–1000 GeV the contribution varies from  $-0.55 \times 10^{-4}$  to  $-1.54 \times 10^{-4}$  for each massless generation of fermions.

# 1 Introduction

The Fermi coupling constant,  $G_F$ , is extracted from the measured value of the muon lifetime,  $\tau_\mu$  via the formula

$$\frac{1}{\tau_\mu} \equiv \Gamma_\mu = \Gamma_0(1 + \Delta q). \quad (1.1)$$

where  $\Delta q$  encapsulates the radiative corrections to all orders in  $\alpha$  as calculated using the lagrangian of the Fermi theory [1–4]. This value of  $G_F$  is then related to the parameters of the Standard Model of electroweak interactions by

$$\frac{G_F}{\sqrt{2}} = \frac{g^2}{8M_W^2}(1 + \Delta r) \quad (1.2)$$

in which  $g$  and  $M_W$  are the renormalized  $SU(2)_L$  coupling constant and  $W$  boson mass, respectively, in whatever renormalization scheme has been chosen.

The quantity  $\Delta r$  was introduced by Sirlin [5] and is intimately related to the  $\rho$ -parameter [6]

$$\rho = \frac{M_W^2}{M_Z^2 \cos^2 \theta_W} = 1 + \delta\rho \quad (1.3)$$

where  $\theta_W$  is the weak mixing angle. For many classes of radiative corrections, generally those that appear only in the  $W$  and  $Z^0$  self-energy diagrams,  $\delta\rho$  is related to  $\Delta r$  by the simple relation,

$$\delta\rho = -\frac{\sin^2 \theta_W}{\cos^2 \theta_W} \Delta r \quad (1.4)$$

Since  $\delta\rho$  was constructed as a way of interrogating the Higgs or mass generation sector of the theory it plays a central rôle in our quest to understand this largely unexplored feature of the Standard Model. This endeavour has already borne fruit. It was the inordinately strong dependence of  $\delta\rho$  on the top quark mass,

$$\delta\rho \sim \left(\frac{\alpha}{4\pi}\right) \frac{3m_t^2}{4M_W^2 \sin^2 \theta_W}, \quad (1.5)$$

that allowed its value to be predicted from precision electroweak data before it was directly observed at the TeVatron [7]. For this reason a great deal of effort has been devoted to calculating classes of 2-loop electroweak corrections contributing to  $\Delta r$  [8–16].

Here the  $\mathcal{O}(N_f \alpha^2)$  corrections to  $\Delta r$  are given. These are the 2-loop corrections containing a massless fermion loop. Since the number of fermions,  $N_f$ , is quite large this class of corrections can be reasonably expected to constitute a dominant subclass.

Moreover the scaling with  $N_f$  provides a unique tag and the complete set of corrections will therefore be gauge-invariant.

This type of enhancement is already seen in the decay widths of the  $W$  and  $Z^0$  bosons that are much broader than typical weak resonances due dominantly to the large number of decay channels available to them. The majority of the  $\mathcal{O}(N_f\alpha^2)$  diagrams that occur in  $\Delta r$  contain the same multiplicative factor, i.e. squares of coupling constants summed over light fermion species, that are responsible for broadening the weak vector bosons.

$\mathcal{O}(N_f\alpha^2)$  corrections have been discussed elsewhere [17] for the self-energy diagrams of the  $W$  and  $Z^0$  at general  $q^2$ . In the present calculation, Feynman diagrams need only be evaluated at  $q^2 = 0$  which simplifies matters considerably and yields much more compact and tractable results. However other classes of diagrams, vertex and box diagrams, now arise. Moreover the complete  $\mathcal{O}(N_f\alpha^2)$  renormalization must be confronted. A detailed study of renormalization at this order was carried out in the context of electric charge renormalization in ref. [18]. In that case the unbroken  $U(1)$  symmetry generates a large number of interrelationships that can be used to test consistency of the renormalization procedure.

In section 2 the notation and conventions used are set out in detail. In general these are identical to those adopted in ref. [18]. In section 3 a brief discussion of Ward identities is given, reviewing the lessons learned from ref. [18] and how they are to be applied to in the present calculation. In section 4 the  $\mathcal{O}(N_f\alpha^2)$  corrections to  $\Delta r^{(2)}$  are given separately for the self-energy, vertex and box contributions. The conclusions arising from the complete analytic result are given in section 5. The appendices contain identities that were used in the course of the calculation along with a complete list of the results for all Feynman diagrams in terms of a single master integral.

## 2 Notation and Conventions

### 2.1 Renormalization

In order to make a physical prediction the complete renormalization of the Standard Model at  $\mathcal{O}(N_f\alpha^2)$  must be carried out. Renormalization at this order has been discussed in detail for a general renormalization scheme in ref. [18] and electromagnetic charge renormalization is considered in particular. This allowed the divergent parts of the  $W$ -fermion vertex to be predicted as explained in section 3.2. The notation adopted here comes directly from ref. [18].

Standard rescalings of the bare  $SU(2)_L$  and  $U(1)$  fields,  $W^0$  and  $B^0$ , are carried out to obtain their associated renormalized fields,  $W$  and  $B$  and wavefunction counterterms,  $\delta Z_W$  and  $\delta Z_B$ . The bare  $SU(2)_L$  and  $U(1)$  coupling constants,  $g^0$  and  $g'^0$ , are treated similarly as are the squares of the bare  $W$  and  $Z$  boson masses,  $(M_W^2)^0$  and  $(M_Z^2)^0$ .

Thus

$$W^0 = (1 + \delta Z_W)^{\frac{1}{2}} W \quad g^0 = g + \delta g \quad (M_W^2)^0 = M_W^2 + \delta M_W^2 \quad (2.1)$$

$$B^0 = (1 + \delta Z_B)^{\frac{1}{2}} B \quad g'^0 = g' + \delta g' \quad (M_Z^2)^0 = M_Z^2 + \delta M_Z^2 \quad (2.2)$$

Expressions for the required counterterms in the charged sector of the theory generated by the substitutions (2.1) and (2.2) are given later in this paper and those for the neutral sector can be found in ref. [18].

The weak mixing angle,  $\theta_W$ , is defined so as to diagonalize the mass matrix of the neutral  $W_3$  and  $B$  fields in the renormalized lagrangian.  $s_\theta$  and  $c_\theta$  are used to denote the sine and cosine of  $\theta_W$  respectively. The relation  $c_\theta^2 = M_W^2/M_Z^2$  then holds exactly in any renormalization scheme provided  $M_W$  and  $M_Z$  are the renormalized masses in the particular renormalization scheme being used.

It is important to note that this choice for  $\theta_W$  is not the only possibility. The weak mixing angle can also be defined so as diagonalize the mass matrix of the bare lagrangian but this will then generate a counterterm,  $\delta\theta_W$ , which is inconvenient and unnecessarily complicated in practice.

In the present calculation it is necessary to distinguish between 1-loop fermionic and bosonic corrections. The order and type of a correction will be indicated, by a superscript in parentheses. Thus  $\delta Z^{(1f)}$  indicates the 1-loop fermionic part of the counterterm  $\delta Z$ . The 1-loop bosonic corrections are denoted by the superscript  $^{(b)}$  and the superscript  $^{(1)}$  indicates both together. The superscript  $^{(2)}$  when used here means the full  $\mathcal{O}(N_f\alpha^2)$  correction.

Throughout this work the Euclidean metric is used with the square of time-like momenta being negative. The calculation is performed in 't Hooft-Feynman,  $R_{\xi=1}$ , gauge.

A fully anti-commuting Dirac  $\gamma_5$  will be assumed. This could only lead to difficulties in fermion loops that generate the antisymmetric  $\epsilon$  tensor, such as internal fermion triangles. Anomaly cancellation in the sum over a complete generation guarantees that additional terms cannot appear. Care must also be taken in the case of external fermion currents where three  $\gamma$  matrices come together. This occurs for the case of box diagrams and will be discussed further in section 4.3.

It was shown in ref. [20] that all  $\mathcal{O}(N_f\alpha^2)$  Feynman diagrams contributing to  $\Delta r^{(2)}$  can be reduced to expressions in terms of the single master integral given in Appendix A.

The calculation was performed in a general renormalization scheme but only results for  $\overline{\text{MS}}$  are presented here. Expressions in this scheme are generally much more compact since the finite parts of counterterms are absent. In addition, for massless fermions, the  $\mathcal{O}(N_f\alpha^2)$  vector-scalar mixing and 2-point scalar counterterms, that could be finite in a general renormalization scheme, vanish. Most of the counterterms required for the calculation of muon decay can be obtained by evaluating 2-loop Feynman diagrams at momentum  $q^2 = 0$ . An exception to this is the  $W$  boson mass counterterm that is obtained from the  $W$  boson self energy evaluated at  $q^2 = -M_W^2$ . In the  $\overline{\text{MS}}$  renor-

malization scheme only the divergent parts are required, however, and these are much easier to calculate than the finite parts.

Renormalization schemes differ only in the finite parts of their counterterms and the so-called on-shell scheme [5] is the most widely-used alternative to  $\overline{\text{MS}}$  in electroweak physics. Explicit expressions for all  $\mathcal{O}(N_f\alpha^2)$  Feynman diagrams that occur in the calculation are given in the appendices. These, of course, do not depend on the renormalization scheme provided the parameters,  $g$ ,  $s_\theta$ ,  $c_\theta$ ,  $M_W$  and  $M_Z$  are interpreted as renormalized parameters in the particular scheme being used. General expressions for the complete set of 1-loop diagrams containing 1-loop counterterms, which are formally of  $\mathcal{O}(N_f\alpha^2)$ , are straightforward if tedious to obtain. They are rather lengthy and so are not given here. Appendix E contains some identities that are useful for the calculation of this class of diagrams where there are counterterm insertions on internal photons and  $Z^0$ 's.

The  $\mathcal{O}(N_f\alpha^2)$  corrections to the muon lifetime in the  $\overline{\text{MS}}$  renormalization scheme constitute one of those rare cases where 2-loop electroweak corrections can be usefully written down. In most other cases the expressions are sufficiently complex that there is little point for them to exist outside of a computer program.

## 2.2 The $\overline{\text{MS}}$ renormalization scheme

The  $\overline{\text{MS}}$  renormalization scheme is implemented in dimensional regularization by requiring that the counterterms contain only pole pieces obtained by Laurent expansion of divergent quantities about  $n = 4$  as they would be under minimal subtraction, MS. Thus a general 2-loop counterterm takes the form,  $\delta Z^{(2)} = a_{-2}\epsilon^{-2} + a_{-1}\epsilon^{-1}$  where  $\epsilon = 2 - n/2$  and  $a_{-2}$  and  $a_{-1}$  are constants. In addition the 't Hooft mass,  $\mu$ , is written in terms of the rescaled  $\mu'$  with  $\mu = (\pi e^\gamma)^{-\frac{1}{2}}\mu'$ . This has the effect of eliminating many of the uninteresting constants that occur at intermediate stages. At 1-loop order this procedure is equivalent to defining the counterterms as being proportional to  $\Delta = \epsilon^{-1} - \gamma - \ln \pi$  but without rescaling the 't Hooft mass.

The exact value that is chosen for  $\mu'$  depends on the particular application that is being considered. For the analysis of electroweak data obtained around the  $Z^0$  resonance  $\mu' = M_Z$  is a reasonable choice since it eliminates the need to resum large logarithms associated with the running of the electromagnetic coupling constant.

## 3 Ward identities

In ref. [18] the  $\mathcal{O}(N_f\alpha^2)$  renormalization of the Standard Model was studied in detail following the prescription of Ross and Taylor [21]. There the gauge-fixing lagrangian is constructed from renormalized, rather than bare, fields in order to satisfy the Ward identities of the theory with the result that the mixing between the vector bosons and Goldstone scalars is no longer completely canceled in  $R_\xi$  gauges. It can be shown that

this is formally equivalent to schemes where the gauge parameter is renormalized [22,23] but is often more convenient to apply in practice. The  $\mathcal{O}(N_f\alpha^2)$  counterterms that mix vectors and scalars are finite in a general renormalization scheme and therefore vanish in the  $\overline{\text{MS}}$  scheme.

Renormalization of the Standard Model has been exhaustively studied at the 1-loop level. There is some flexibility as to whether wavefunction counterterms,  $\delta Z^{(1)}$  are used or not. If they are employed the Green's functions are rendered finite but the wavefunction counterterms cancel out when the Green's functions are combined to form physical  $S$ -matrix elements. This is demonstrated in Appendix E. It follows that the wavefunction counterterms can be dropped altogether, for example see ref. [5], provided one is prepared to deal with divergent Green's functions. The divergences will then cancel out in overall physical matrix elements. In practice this feature provides a useful check of the calculation.

In ref. [18] it was shown that at 2-loop order the wavefunction counterterms,  $\delta Z^{(2)}$  cancel in physical matrix elements, and so can be dropped if desired, but that the 1-loop wavefunction counterterms must be included in a manner consistent with the 1-loop Ward identities

$$\frac{1}{2}\delta Z_B^{(1)} + \frac{\delta g^{(1)}}{g'} = 0 \quad (3.1)$$

$$\frac{1}{2}\delta Z_W^{(1f)} + \frac{\delta g^{(1f)}}{g} = 0 \quad (3.2)$$

where eq.(3.1) is true for both fermionic and bosonic counterterms separately.

The imposition of the Ward identities, (3.1) and (3.2), leads to some quite substantial simplifications. Further simplification can also be obtained by noting that in any renormalization scheme

$$\frac{1}{2}\delta Z_W^{(1b)} + \frac{\delta g^{(1b)}}{g} + 2 \left( \frac{g^2}{16\pi^2} \right) (\pi M_W^2)^{-\epsilon} \Gamma(\epsilon) = \text{finite} \quad (3.3)$$

$$\delta Z_\phi^{(1f)} = \frac{\delta M_W^{2(1f)}}{M_W^2} - 2 \frac{\delta g^{(1f)}}{g} = \text{finite} \quad (3.4)$$

The former vanishes in the on-shell renormalization scheme and the latter in  $\overline{\text{MS}}$ . Here  $\delta Z_\phi$  is the wavefunction counterterm for the Higgs field.

## 4 The $\mathcal{O}(N_f\alpha^2)$ Corrections to $\Delta r^{(2)}$

### 4.1 The $W$ -boson Self-Energy

The Feynman diagrams contributing to the  $W$ -boson self-energy at  $\mathcal{O}(N_f\alpha^2)$  are shown in Fig.2. Internal lines labeled  $Z,\gamma$  mean that all allowable combinations must be included.

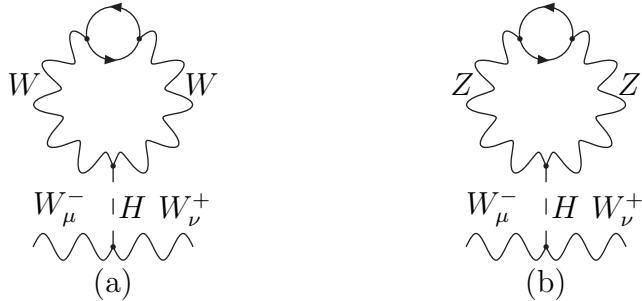


Figure 1:  $\mathcal{O}(N_f\alpha^2)$  tadpole diagrams contributing to the  $W$  boson self energy.

For the present case of zero external momentum,  $q = 0$ , the vector boson self-energies,  $\Pi_{\mu\nu}(q^2)$ , can only take the form

$$\Pi_{\mu\nu}(0) = \delta_{\mu\nu} F$$

where  $F$  is a function of the internal masses only and may be obtained from the tensor integral representation of  $\Pi_{\mu\nu}(0)$  by means of the projection operator,  $\delta_{\mu\nu}/n$ . Thus

$$F = \left( \frac{\delta_{\mu\nu}}{n} \right) \Pi_{\mu\nu}(0). \quad (4.1)$$

The resulting scalar integral can always be written in terms of the master integral,  $I_0(j, k, l, m, n, M^2)$ , of eq.(A.6) and the results are exact for all  $n$ .

Tadpole diagrams that can appear in the  $W$  self-energy at  $\mathcal{O}(N_f\alpha^2)$  are shown in Fig.1. At this order the individual diagrams are gauge-invariant and they are the only contributions  $\propto M_H^{-2}$  where  $M_H$  is the Higgs mass. In some renormalization schemes it is possible to eliminate them by a suitable choice of the tadpole counterterm,  $\delta\beta$ , however in a strictly  $\overline{\text{MS}}$  calculation this is not an option. The finite parts of tadpole diagrams are not expected to enter strongly into physical results since they represent a universal shift in the Higgs vacuum expectation value and thus they have not been included with the other corrections.

Since the Higgs mass is now known to satisfy,  $M_H > M_W$ , one may define, for notational convenience,  $c_h^2 = 1 - M_W^2/M_H^2$  and  $s_h^2 = 1 - c_h^2$  in analogy with  $c_\theta$  and  $s_\theta$ .

Fig.2(c), along with associated counterterm diagrams, is the only topology in which the physical Higgs particle occurs. In the  $\overline{\text{MS}}$  renormalization scheme the 1-loop counterterm insertions in 1-loop diagrams containing the Higgs vanish when taken together. Fig.2(c) therefore accounts for the full  $M_H$  dependence in  $\Delta r^{(2)}$ . In order to obtain the  $\mathcal{O}(N_f\alpha^2)$   $W$  boson mass counterterm,  $\delta M_W^{2(2)}$ , the  $W$  boson self-energy,  $\Pi_{WW}(q^2)$  needs to be evaluated at  $q^2 = -M_W^2$ . In contrast the other  $\mathcal{O}(N_f\alpha^2)$  counterterms that occur in the calculation can be gotten from Feynman diagrams evaluated at  $q^2 = 0$ . In principle  $\Pi_{WW}^{(2)}(-M_W^2)$  could be obtained in its entirety by the methods described

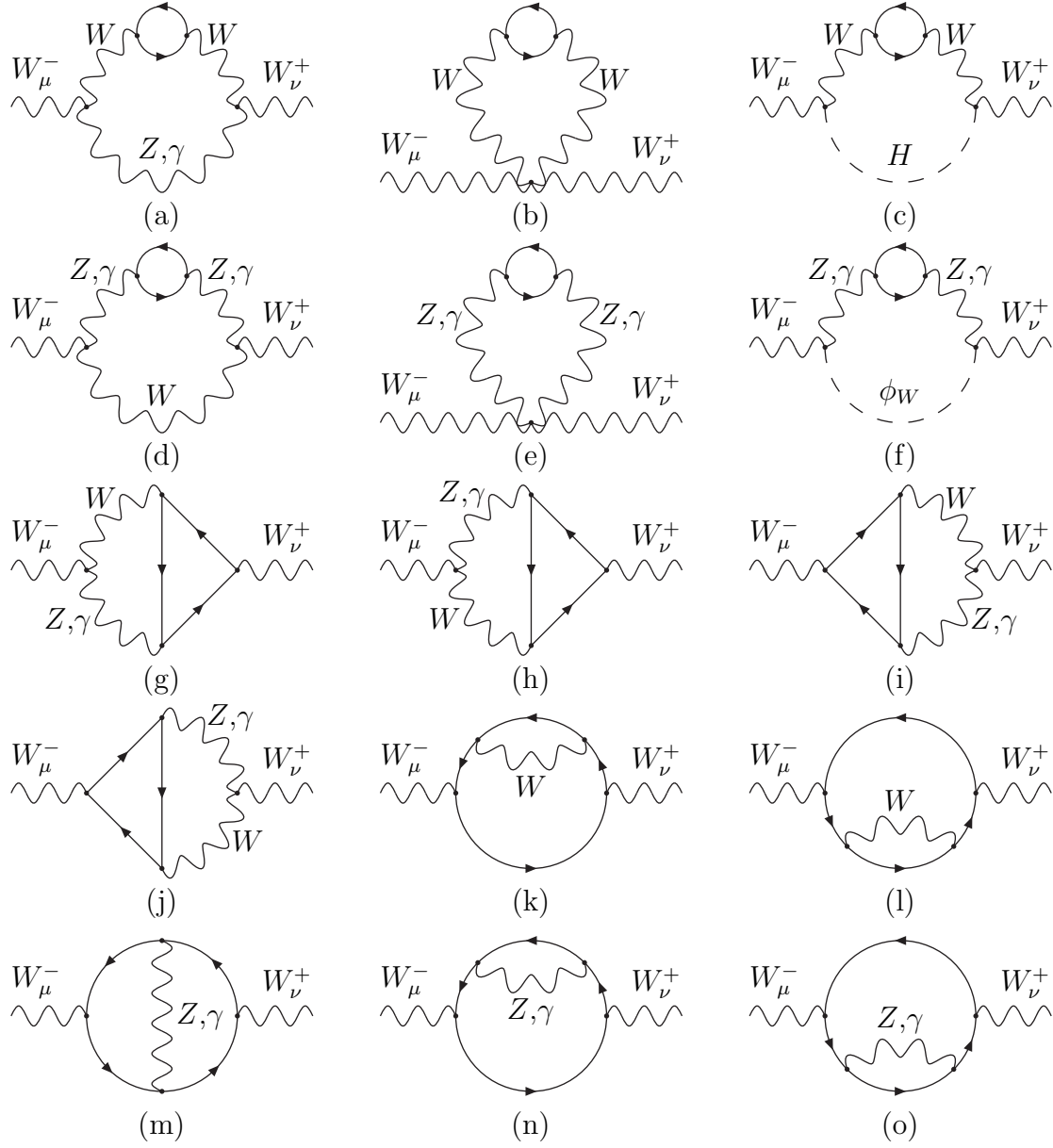


Figure 2:  $\mathcal{O}(N_f \alpha^2)$  Feynman diagrams contributing to the  $W$  boson self energy.



in refs [17, 24] however in the  $\overline{\text{MS}}$  renormalization scheme only its divergent pieces are needed and these are considerably easier to extract and yield much more manageable expressions. Suffice it to say that they contain both local pieces, proportional to polynomials in  $q^2$  and non-local pieces proportional to  $\ln q^2$ ,  $\ln(q^2 + M_W^2)$  etc. When combined with 1-loop diagrams in which 1-loop counterterms have been inserted the non-local divergences must cancel so that the remaining divergences can be removed by purely local  $\mathcal{O}(N_f\alpha^2)$  counterterms. This cancellation occurs between several diagrams and provides a stringent check of relative signs and combinatoric factors.

The diagrams involving an internal photon require additional care due to the fact that the integrals encounter singularities in certain limits of interest for the external momenta. Such diagrams were evaluated by introducing a small mass term for the photon and then taking the limit in an appropriate order. In the diagrams of Fig.2(a)&(d),  $q^2 = -M_W^2$  is a branch point and the integral blows up when evaluated naïvely. In that case the photon mass is set to zero only after taking the limit  $q \rightarrow -M_W^2$ . Further checks on the procedure were obtained by evaluating the diagrams in various regions of momentum space with and without the photon mass term; for example, the  $q \rightarrow 0$  limits were checked against the same diagrams evaluated by setting  $q = 0$  at the outset.

At  $\mathcal{O}(N_f\alpha^2)$  the 2-point  $W$  counterterm is

$$\begin{aligned} \text{Diagram} &= - (q^2 + M_W^2) \delta Z_W^{(2)} \delta_{\mu\nu} - \delta Z_W^{(2)} q_\mu q_\nu - \delta M_W^{2(2)} \delta_{\mu\nu} \\ &\quad - \left( \delta Z_W^{(1f)} \delta M_W^{2(1b)} + \delta Z_W^{(1b)} \delta M_W^{2(1f)} \right) \delta_{\mu\nu}. \end{aligned}$$

The  $W$  boson self-energy enters  $\Delta r$  via the relation  $\Delta r_{\text{SE}}^{(2)} = \Pi_{WW}^{(2)}(0)/M_W^2$ . For one complete generation of massless fermions the  $\mathcal{O}(N_f\alpha^2)$  diagrams containing the physical Higgs, Fig.2(c), gives

$$\begin{aligned} \Delta r_{\text{SEH}}^{(2)} = - \left( \frac{g^2}{16\pi^2} \right)^2 \left\{ \frac{(20 + s_h^2 + 2\pi^2 s_h^2)}{8s_h^2} - \frac{(4 + s_h^2)}{2s_h^2} \ln \frac{M_W^2}{\mu'^2} \right. \\ \left. - \frac{\ln c_h^2}{s_h^4} \left( \ln \frac{M_W^2}{\mu'^2} + \ln \frac{M_H^2}{\mu'^2} - \frac{5}{2} \right) + \ln^2 \frac{M_W^2}{\mu'^2} \right\} \quad (4.2) \end{aligned}$$

After combining the  $\mathcal{O}(N_f\alpha^2)$  diagrams of Fig.2 with 1-loop diagrams that contain 1-loop counterterm insertions the result is

$$\begin{aligned} \Delta r_{\text{SEW}}^{(2)} = \left( \frac{g^2}{16\pi^2} \right)^2 \left\{ \frac{(1158 - 3496s_\theta^2 + 2803s_\theta^4 - 480s_\theta^6)}{72c_\theta^4} + \frac{(4 - 8s_\theta^2 - s_\theta^4)}{12c_\theta^4} \pi^2 \right. \\ \left. + \frac{(294 - 529s_\theta^2)}{18s_\theta^2} \ln c_\theta^2 - \frac{(12 - 23s_\theta^2)}{3s_\theta^2} \left( \ln c_\theta^2 + 2 \ln \frac{M_Z^2}{\mu'^2} \right) \ln c_\theta^2 \right. \\ \left. - \frac{(50 - 156s_\theta^2 + 117s_\theta^4 - 16s_\theta^6)}{6c_\theta^4} \ln \frac{M_Z^2}{\mu'^2} + \frac{(3 - 6s_\theta^2 - 2s_\theta^4)}{3c_\theta^4} \ln^2 \frac{M_Z^2}{\mu'^2} \right\} \quad (4.3) \end{aligned}$$

As noted above the divergences that remained have been shown to be purely local and have been removed in a manner consistent with  $\overline{\text{MS}}$  renormalization.

## 4.2 Vertex Corrections

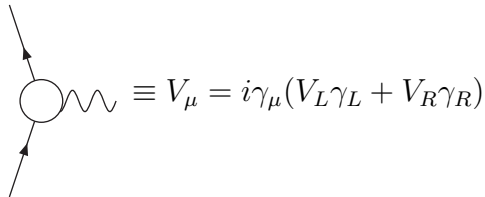
The  $\mathcal{O}(N_f\alpha^2)$  vertex diagrams and external leg corrections contributing to  $\Delta r^{(2)}$  are shown in Fig.3.

The diagrams of Fig.3 containing only virtual photons are IR divergent and must be separated into UV finite, IR divergent QED corrections that are already included by  $\Delta q$  in the extraction of  $G_F$  [3]. Sirlin [5, 25, 26] has described a strategy that, starting from the full electroweak theory, makes the separation of contributions to  $\Delta q$  and  $\Delta r$  automatic at least up to  $\mathcal{O}(\alpha m_\mu^2/M_W^2)$ . In diagrams exhibiting infrared (IR) divergences, the photon propagator is replaced by

$$\frac{1}{k^2} \longrightarrow \left\{ \frac{1}{k^2} - \frac{1}{k^2 + \Lambda^2} \right\} + \frac{1}{k^2 + \Lambda^2}. \quad (4.4)$$

where it is generally convenient to take  $\Lambda = M_W$ . The term in curly brackets is simply the original photon propagator with a Pauli-Villars regulator. It has the same IR behaviour and gives contributions that are identical to those of Fermi theory up to  $\mathcal{O}(\alpha m_\mu^2/M_W^2)$  and thus are contained in  $\Delta q$ . The second term in (4.4) gives contributions that retain the original UV behaviour but are free from IR singularities and therefore belong in  $\Delta r$ . The UV divergent, IR finite weak corrections that are included in  $\Delta r^{(2)}$  are, as already pointed out in ref. [4], independent of the separation mass,  $\Lambda$ , because of a cancellation against corresponding 1-loop diagrams with 1-loop counterterm insertions.

For processes with massless external fermions the only relevant vertex corrections are those involving vector bosons and these will necessarily be purely vector and axial-vector in character. A general vertex correction can then be represented as



$$\text{Diagram} \equiv V_\mu = i\gamma_\mu(V_L\gamma_L + V_R\gamma_R)$$

where  $V_L$  and  $V_R$  are functions only of the internal masses. The tensor integral representation of  $V_\mu$  can easily be obtained by standard techniques and from it the scalar integral representations of  $V_L$  and  $V_R$  follow by means of projection operators. Thus

$$V_{L,R} = -\frac{i}{2n} \text{Tr}\{V_\mu\gamma_\mu\gamma_{R,L}\}. \quad (4.5)$$

where  $\text{Tr}\{\gamma_\mu\gamma_\mu\} = 4n$  is assumed. This method for directly obtaining the scalar integral representation of the vertex form factors is particularly convenient when computer algebra is being employed. Once again the resulting scalar integrals can be written in terms of the master integral,  $I_0(j, k, l, m, n, M^2)$ . of eq.(A.6).

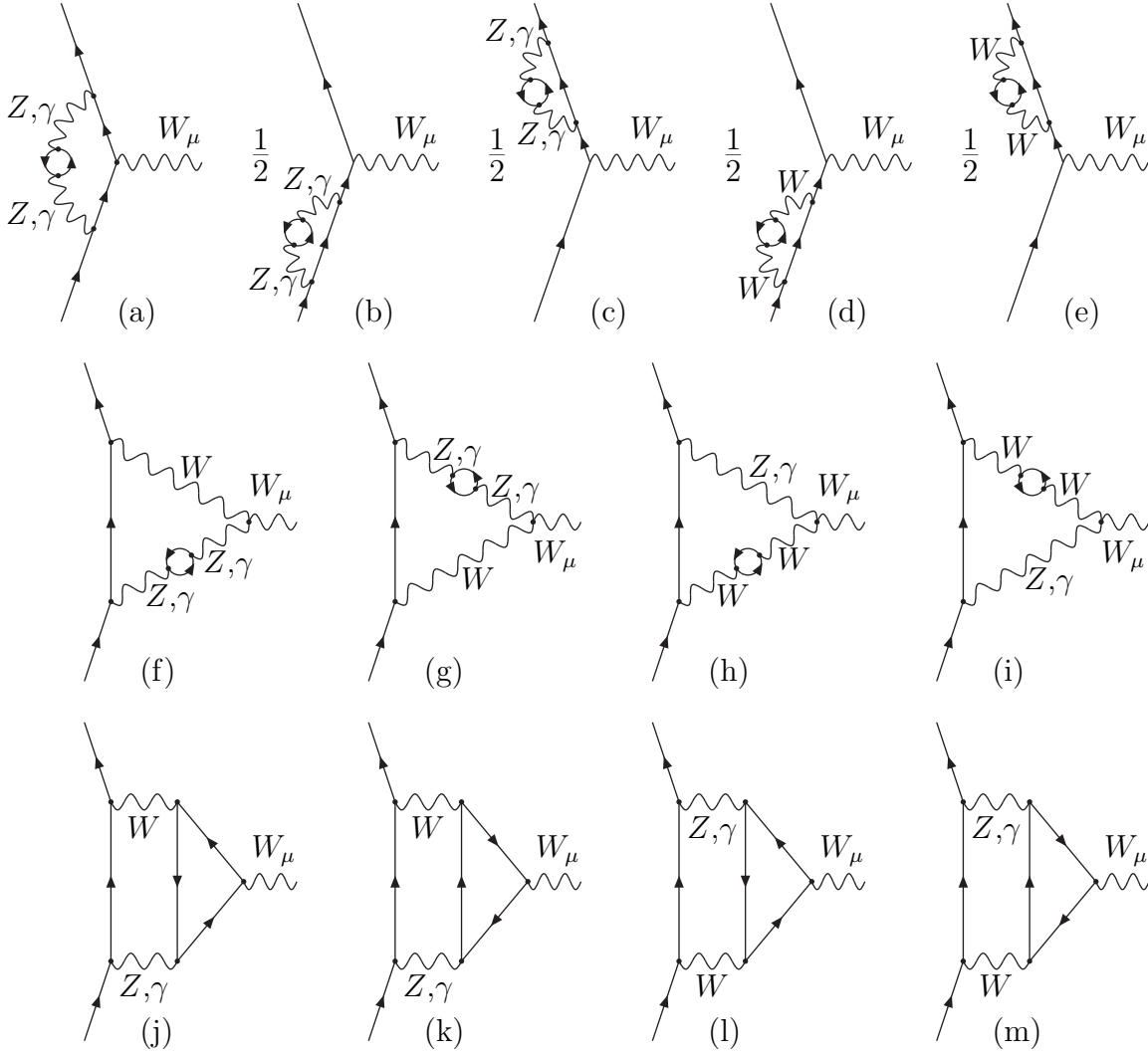
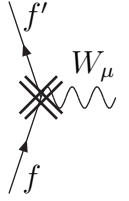


Figure 3:  $\mathcal{O}(N_f \alpha^2)$  vertex and external leg corrections contributing to muon decay.

The  $\mathcal{O}(N_f\alpha^2)$   $Wff'$  vertex counterterm is given by



$$= i \frac{g}{\sqrt{2}} \gamma_\mu \gamma_L \left\{ \frac{1}{2} \delta Z_W^{(2)} + \frac{\delta g^{(2)}}{g} + 2 \frac{\delta g^{(1f)}}{g} \left( \frac{1}{2} \delta Z_W^{(1b)} + \frac{\delta g^{(1b)}}{g} \right) - 3 \frac{\delta g^{(1f)}}{g} \cdot \frac{\delta g^{(1b)}}{g} \right\} \quad (4.6)$$

In ref. [18] it was shown, by considering electric charge renormalization, that in any renormalization scheme the  $\mathcal{O}(N_f\alpha^2)$  counterterms must satisfy the relation

$$\begin{aligned} & \frac{1}{2} \delta Z_W^{(2)} + \frac{\delta g^{(2)}}{g} + 2 \frac{\delta g^{(1f)}}{g} \left( \frac{1}{2} \delta Z_W^{(1b)} + \frac{\delta g^{(1b)}}{g} \right) - 3 \frac{\delta g^{(1b)}}{g} \cdot \frac{\delta g^{(1f)}}{g} \\ &= \left( \frac{g^2}{16\pi^2} \right)^2 8 \frac{(\pi M_W^2)^{n-4}}{n} \Gamma(4-n) \Gamma\left(2 - \frac{n}{2}\right) \Gamma\left(\frac{n}{2}\right) \\ & \quad - 3 \frac{\delta g^{(1f)}}{g} \left( \frac{g^2}{16\pi^2} \right) (\pi M_W^2)^{-\epsilon} \Gamma(\epsilon) + \frac{\delta M_W^{2(1f)}}{M_W^2} \left( \frac{g^2}{16\pi^2} \right) (\pi M_W^2)^{-\epsilon} \Gamma(\epsilon) + \text{finite} \end{aligned} \quad (4.7)$$

from which expressions for the  $\overline{\text{MS}}$  counterterms on the left hand side of Eq.(4.7) are easily extracted giving

$$\frac{1}{2} \delta Z_W^{(2)} + \frac{\delta g^{(2)}}{g} + 2 \frac{\delta g^{(1f)}}{g} \left( \frac{1}{2} \delta Z_W^{(1b)} + \frac{\delta g^{(1b)}}{g} \right) - 3 \frac{\delta g^{(1b)}}{g} \cdot \frac{\delta g^{(1f)}}{g} = -\frac{1}{\epsilon^2} + \frac{5}{6\epsilon}. \quad (4.8)$$

When the weak parts of the Feynman diagrams of Fig.3, obtained by means of eq.(4.4), are combined with the 1-loop diagrams with  $\mathcal{O}(N_f\alpha)$  counterterm insertions and the  $\mathcal{O}(N_f\alpha^2)$  counterterms (4.8) the result is indeed finite. This provides not only a check of the calculation performed here but also of overall renormalization prescription as performed in ref. [18]. The vertex and external leg corrections for a complete generation of massless fermions contribute

$$\begin{aligned} \Delta r_{\text{vertex}}^{(2)} &= - \left( \frac{g^2}{16\pi^2} \right)^2 \left\{ \frac{2\pi^2}{3} + \frac{5}{6} (17 - 32s_\theta^2) + \frac{4(11 - 27s_\theta^2)}{3s_\theta^2} \ln c_\theta^2 \right. \\ & \quad \left. - \frac{16}{3} (2 - 3s_\theta^2) \ln \frac{M_Z^2}{\mu'^2} - \frac{(5 - 12s_\theta^2)}{s_\theta^2} \left( \ln c_\theta^2 + 2 \ln \frac{M_Z^2}{\mu'^2} \right) \ln c_\theta^2 + 2 \ln^2 \frac{M_Z^2}{\mu'^2} \right\} \end{aligned} \quad (4.9)$$

### 4.3 Box Diagrams

The  $\mathcal{O}(N_f\alpha^2)$  box diagrams contributing to muon decay are shown in Fig.4. Other box diagrams can be constructed in which the internal bosons cross but these all vanish

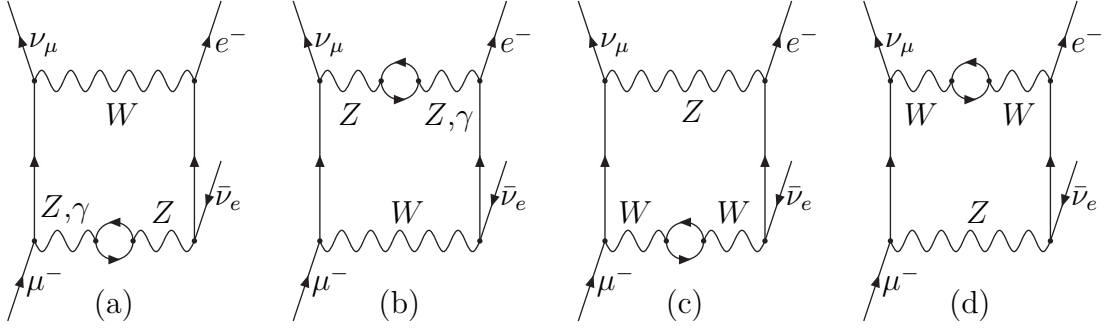


Figure 4:  $\mathcal{O}(N_f\alpha^2)$  box diagrams contributing to muon decay. Other box diagrams that can be constructed vanish.

identically because they are proportional to products of the left-handed with right-handed couplings of the  $W$  for which the latter is zero. The only IR divergent box diagram, that contains an internal photon, vanishes in this way and so the procedure for separating QED and weak corrections (4.4) does not need to be invoked. All diagrams are only logarithmically divergent with simple poles at  $n = 4$ .

The box diagrams containing a virtual photon and a counterterm insertion on the  $W$  propagator can also, in principle, produce IR divergent contributions that would require the separation strategy (4.4) to be invoked but

$$\begin{aligned}
 & \text{Diagram 1} + \text{Diagram 2} + \text{Diagram 3} = \left( 2\frac{\delta g^{(1f)}}{g} - \frac{\delta M_W^{2(1f)}}{M_W^2} \right) \text{Diagram 4} \\
 & \hspace{15em} (4.10)
 \end{aligned}$$

and in the  $\overline{\text{MS}}$  renormalization scheme the combination of counterterms on the right hand side of Eq.(4.10) vanishes.

For 4-fermion processes one-loop box diagrams are finite but at  $\mathcal{O}(N_f\alpha^2)$  they develop logarithmic divergences. A useful set of identities for calculating one-loop box diagrams appears in ref. [27]. They are, however, valid only for  $n = 4$  because of their intended use at one-loop. The relations involve products of strings of three  $\gamma$  matrices and care must be taken in applying and generalizing identities like

$$\gamma_\rho\gamma_\alpha\gamma_\sigma = \delta_{\rho\alpha}\gamma_\sigma - \delta_{\rho\sigma}\gamma_\alpha + \delta_{\alpha\sigma}\gamma_\rho - \epsilon_{\rho\alpha\sigma\beta}\gamma_\beta\gamma_5. \quad (4.11)$$

It should be noted that at  $\mathcal{O}(N_f\alpha^2)$  the box diagrams contain only simple poles at  $n = 4$  and are rendered finite by  $\mathcal{O}(\alpha)$  counterterms inserted into finite 1-loop diagrams. The details of the convention adopted in treating terms proportional to  $(n-4)$  cancel and are therefore irrelevant for the present purposes. The only requirement is that a consistent convention be adopted. For definiteness we take

$$[\gamma_\rho\gamma_\mu\gamma_\sigma\gamma_{L,R}]_1[\gamma_\rho\gamma_\nu\gamma_\sigma\gamma_{L,R}]_2 = 4\delta_{\mu\nu}[\gamma_\alpha\gamma_{L,R}]_1[\gamma_\alpha\gamma_{L,R}]_2 + (n-4)[\gamma_\mu\gamma_{L,R}]_1[\gamma_\nu\gamma_{L,R}]_2 \quad (4.12)$$

$$[\gamma_\rho\gamma_\mu\gamma_\sigma\gamma_{L,R}]_1[\gamma_\rho\gamma_\nu\gamma_\sigma\gamma_{R,L}]_2 = 4[\gamma_\nu\gamma_{L,R}]_1[\gamma_\mu\gamma_{R,L}]_2 + (n-4)[\gamma_\mu\gamma_{L,R}]_1[\gamma_\nu\gamma_{R,L}]_2 \quad (4.13)$$

$$[\gamma_\rho\gamma_\mu\gamma_\sigma\gamma_{L,R}]_1[\gamma_\sigma\gamma_\nu\gamma_\rho\gamma_{L,R}]_2 = 4[\gamma_\nu\gamma_{L,R}]_1[\gamma_\mu\gamma_{L,R}]_2 + (n-4)[\gamma_\mu\gamma_{L,R}]_1[\gamma_\nu\gamma_{L,R}]_2 \quad (4.14)$$

$$[\gamma_\rho\gamma_\mu\gamma_\sigma\gamma_{L,R}]_1[\gamma_\sigma\gamma_\nu\gamma_\rho\gamma_{R,L}]_2 = 4\delta_{\mu\nu}[\gamma_\alpha\gamma_{L,R}]_1[\gamma_\alpha\gamma_{R,L}]_2 + (n-4)[\gamma_\mu\gamma_{L,R}]_1[\gamma_\nu\gamma_{R,L}]_2 \quad (4.15)$$

where the square brackets  $[ ]_1$  and  $[ ]_2$  indicate that the enclosed  $\gamma$ -matrices are associated with the external fermion currents  $J_1$  and  $J_2$  respectively.

The general  $\mathcal{O}(N_f\alpha^2)$  box diagram for massless external fermions at  $q = 0$  therefore takes the form

$$B_{\mu\nu}J_{1\mu}J_{2\nu} = B \cdot J_{1\alpha}J_{2\alpha}. \quad (4.16)$$

Here  $B_{\mu\nu}$  is a tensor integral and the product of  $J_{1\alpha}J_{2\alpha}$  can be constructed from one or a combination of the  $\gamma$ -matrices appearing in eq.(4.12)–(4.15). As for the self-energy contributions, the tensor integral  $B_{\mu\nu}$ , can only be proportional to  $\delta_{\mu\nu}$  and hence, using the projection operator method of section 4.1, the scalar integral representation for the form factor  $B$  is seen to be  $B = (\delta_{\mu\nu}/n)B_{\mu\nu} = B_{\mu\mu}/n$ . In this case the identities (4.12)–(4.15) simplify to become

$$\frac{\delta_{\mu\nu}}{n}[\gamma_\rho\gamma_\mu\gamma_\sigma\gamma_{L,R}]_1[\gamma_\rho\gamma_\nu\gamma_\sigma\gamma_{L,R}]_2 = \frac{(5n-4)}{n}[\gamma_\alpha\gamma_{L,R}]_1[\gamma_\alpha\gamma_{L,R}]_2 \quad (4.17)$$

$$\frac{\delta_{\mu\nu}}{n}[\gamma_\rho\gamma_\mu\gamma_\sigma\gamma_{L,R}]_1[\gamma_\rho\gamma_\nu\gamma_\sigma\gamma_{R,L}]_2 = [\gamma_\alpha\gamma_{L,R}]_1[\gamma_\alpha\gamma_{R,L}]_2 \quad (4.18)$$

$$\frac{\delta_{\mu\nu}}{n}[\gamma_\rho\gamma_\mu\gamma_\sigma\gamma_{L,R}]_1[\gamma_\sigma\gamma_\nu\gamma_\rho\gamma_{L,R}]_2 = [\gamma_\alpha\gamma_{L,R}]_1[\gamma_\alpha\gamma_{L,R}]_2 \quad (4.19)$$

$$\frac{\delta_{\mu\nu}}{n}[\gamma_\rho\gamma_\mu\gamma_\sigma\gamma_{L,R}]_1[\gamma_\sigma\gamma_\nu\gamma_\rho\gamma_{R,L}]_2 = \frac{(5n-4)}{n}[\gamma_\alpha\gamma_{L,R}]_1[\gamma_\alpha\gamma_{R,L}]_2. \quad (4.20)$$

When the diagrams of Fig.4 are combined with 1-loop box diagrams, in which 1-loop fermionic  $\overline{\text{MS}}$  counterterms have been inserted in all possible ways, the result was found to be finite and give a contribution to  $\Delta r^{(2)}$  of

$$\Delta r_{\text{box}}^{(2)} = -2 \left( \frac{g^2}{16\pi^2} \right)^2 \left\{ \frac{(3-8s_\theta^2)(1-2s_\theta^2)}{3c_\theta^2} \left( \ln \frac{M_Z^2}{\mu'^2} - \frac{5}{3} \right) - \frac{(21-52s_\theta^2)}{9s_\theta^2} \ln c_\theta^2 \right. \\ \left. + \frac{(3-7s_\theta^2)}{3s_\theta^2} \left( \ln c_\theta^2 + 2 \ln \frac{M_Z^2}{\mu'^2} \right) \ln c_\theta^2 \right\} \quad (4.21)$$

## 5 Conclusions

Combining the contributions from  $W$  self energy corrections given in Eq.(4.2) and Eq.(4.3) with the vertex corrections of Eq.(4.9) and box diagram corrections of Eq.(4.21) for one complete massless generation of fermions finally gives

$$\begin{aligned} \Delta r^{(2)} = & - \left( \frac{g^2}{16\pi^2} \right)^2 \left\{ \frac{5}{2s_h^2} - \frac{2}{s_h^2} \ln \frac{M_W^2}{\mu'^2} - \frac{\ln c_h^2}{s_h^4} \left( \ln \frac{M_W^2}{\mu'^2} + \ln \frac{M_H^2}{\mu'^2} - \frac{5}{2} \right) \right. \\ & - \frac{(369 - 878s_\theta^2 + 334s_\theta^4 + 160s_\theta^6)}{72c_\theta^4} + \frac{(7 - 14s_\theta^2 + 12s_\theta^4)}{12c_\theta^4} \pi^2 \\ & - \frac{(57 - 40s_\theta^2)}{9s_\theta^2} \ln c_\theta^2 + \frac{(3 + 2s_\theta^2)}{3s_\theta^2} \left( \ln c_\theta^2 + 2 \ln \frac{M_Z^2}{\mu'^2} \right) \ln c_\theta^2 \\ & \left. - \frac{(5 - 6s_\theta^2 + 22s_\theta^4 - 16s_\theta^6)}{6c_\theta^4} \ln \frac{M_Z^2}{\mu'^2} + \frac{(6 - 12s_\theta^2 + 11s_\theta^4)}{3c_\theta^4} \ln^2 \frac{M_Z^2}{\mu'^2} \right\} \quad (5.1) \end{aligned}$$

which obviously simplifies substantially for  $\mu' = M_Z$ . Upon evaluation one finds, for a 't Hooft mass  $\mu' = 91.1867 \text{ GeV}$  that  $\Delta r^{(2)} = -5.45 \times 10^{-5}$ ,  $-7.28 \times 10^{-5}$  and  $-1.54 \times 10^{-4}$  for  $M_H = 100 \text{ GeV}$ ,  $300 \text{ GeV}$  and  $1000 \text{ GeV}$  respectively.  $s_\theta$  was set to its corresponding  $\overline{\text{MS}}$  values of 0.2316, 0.2322 and 0.2330 obtained from the program ZOPOLE [29].

For physics on or above the  $Z^0$  resonance, the number of light generations is at least 2 and could be taken to be 3 depending on exactly how the top quark mass corrections are to be treated. The correction is large compared with what would be expected for a 2-loop electroweak correction and therefore clearly displays the enhancement with the fermion number,  $N_f$ .

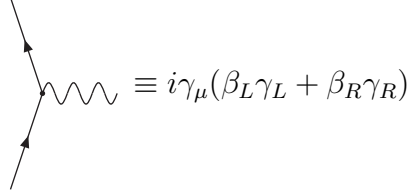
As mentioned in the introduction, a number of classes of 2-loop contributions to  $\Delta r$  have now been computed. Few, if any, dominant classes remain to be tackled and the next logical step is the complete set of 2-loop corrections. In order to use these in making theoretical predictions the full renormalization of the Standard Model at 2-loop order would be required. Many of the issues that need to be confronted in undertaking the full renormalization have been encountered in this work and in ref. [18].

## Acknowledgments

RGS wishes to thank the Max-Planck-Institut für Physik, Munich, for hospitality while part of this work was carried out. This work was supported in part by the US Department of Energy.

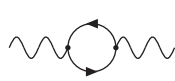
## A The Master Integral

If the general coupling of a fermion to a vector boson will be denoted



$$\equiv i\gamma_\mu(\beta_L\gamma_L + \beta_R\gamma_R)$$

where  $\gamma_L$  and  $\gamma_R$  are the usual left- and right-handed helicity projection operators and  $\beta_L$  and  $\beta_R$  are the corresponding coupling constants then the  $\mathcal{O}(N_f\alpha^2)$  diagrams that are obtained from 1-loop diagrams by the insertion of a massless fermion loop into an internal vector boson line are most easily calculated by means of the following identity. For the massless fermion loop insertion, it may be shown that



$$= - \left( \delta_{\mu\nu} - \frac{p_\mu p_\nu}{p^2} \right) \frac{(\beta_L\beta'_L + \beta_R\beta'_R)}{16\pi^2} \frac{(n-2)}{(n-1)} \int \frac{d^n q}{i\pi^2} \frac{p^2}{q^2(q+p)^2} \quad (\text{A.1})$$

$$= - (p^2\delta_{\mu\nu} - p_\mu p_\nu) \frac{(\beta_L\beta'_L + \beta_R\beta'_R)}{16\pi^2} 4(\pi p^2)^{\frac{n}{2}-2} \frac{\Gamma^2\left(\frac{n}{2}\right)}{\Gamma(n)} \Gamma\left(2 - \frac{n}{2}\right) \quad (\text{A.2})$$

where  $\beta_L$ ,  $\beta_R$  and  $\beta'_L$ ,  $\beta'_R$  are the couplings of the attached vector bosons.

The master integral, to which all  $\mathcal{O}(N_f\alpha^2)$  diagrams relevant for the present calculation can be reduced, takes the form

$$I(j, k, l, m, n, M^2) = \int \frac{d^n p}{i\pi^2} \frac{1}{[p^2]^j [p^2 + M^2]^k} \int \frac{d^n q}{i\pi^2} \frac{1}{[q^2]^l [(q+p)^2]^m}. \quad (\text{A.3})$$

In eq.(A.3), the integration over  $q$  can be performed using standard Feynman parameter techniques and yields

$$\int \frac{d^n q}{i\pi^2} \frac{1}{[q^2]^l [(q+p)^2]^m} = \frac{\pi^{\frac{n}{2}-2}}{[p^2]^{l+m-\frac{n}{2}}} \frac{\Gamma\left(l+m-\frac{n}{2}\right) \Gamma\left(\frac{n}{2}-l\right) \Gamma\left(\frac{n}{2}-m\right)}{\Gamma(l)\Gamma(m)\Gamma(n-l-m)}. \quad (\text{A.4})$$

The resulting integral with respect to  $p$  in eq.(A.3) is independent of angle and hence

$$\begin{aligned} \int \frac{d^n p}{i\pi^2} \frac{1}{[p^2]^{j+l+m-\frac{n}{2}} [p^2 + M^2]^k} &= \frac{2\pi^{\frac{n}{2}-2}}{\Gamma\left(\frac{n}{2}\right)} \int_0^\infty dp \frac{p^{2n-2j-2l-2m-1}}{[p^2 + M^2]^k} \\ &= \frac{\pi^{\frac{n}{2}-2}}{(M^2)^{k+j+l+m-n}} \frac{\Gamma(n-j-l-m)\Gamma(k+j+l+m-n)}{\Gamma\left(\frac{n}{2}\right)\Gamma(k)} \end{aligned} \quad (\text{A.5})$$



from which it follows

$$\begin{aligned}
I_0(j, k, l, m, n, M^2) &= \frac{\pi^{n-4}}{(M^2)^{k+j+l+m-n}} \\
&\times \frac{\Gamma(n-j-l-m)\Gamma(k+j+l+m-n)\Gamma\left(l+m-\frac{n}{2}\right)\Gamma\left(\frac{n}{2}-l\right)\Gamma\left(\frac{n}{2}-m\right)}{\Gamma\left(\frac{n}{2}\right)\Gamma(k)\Gamma(l)\Gamma(m)\Gamma(n-l-m)}
\end{aligned} \tag{A.6}$$

For the purposes of compactness it is useful to define the related integrals

$$I_1(j, n, M_1^2, M_2^2) = \int \frac{d^n p}{i\pi^2} \frac{1}{[p^2]^j [p^2 + M_1^2][p^2 + M_2^2]} \int \frac{d^n q}{i\pi^2} \frac{1}{q^2(q+p)^2} \tag{A.7}$$

$$= \frac{1}{(M_1^2 - M_2^2)} \{I_0(j, 1, 1, 1, n, M_2^2) - I_0(j, 1, 1, 1, n, M_1^2)\} \tag{A.8}$$

and

$$I_2(j, n, M_1^2, M_2^2) = \int \frac{d^n p}{i\pi^2} \frac{1}{[p^2]^j [p^2 + M_1^2][p^2 + M_2^2]^2} \int \frac{d^n q}{i\pi^2} \frac{1}{q^2(q+p)^2} \tag{A.9}$$

$$\begin{aligned}
&= \frac{1}{(M_1^2 - M_2^2)^2} \{I_0(j, 1, 1, 1, n, M_1^2) \\
&\quad + (M_1^2 - M_2^2)I_0(j, 2, 1, 1, n, M_2^2) - I_0(j, 1, 1, 1, n, M_2^2)\}
\end{aligned} \tag{A.10}$$

Finally, the  $q \neq 0$  amplitudes were obtained independently and required varied and extensive techniques and will appear in a separate publication [19].

## B $W$ Self Energy Corrections

In this appendix the contributions from individual Feynman diagrams to the  $\mathcal{O}(N_f \alpha^2)$   $W$  boson self-energy,  $\Pi_{WW}^{(2)}(0)$ , are listed. Their net effect on the inverse muon lifetime,  $\Gamma^{(0)} = g^4 m_\mu^5 / (6144 \pi^3 M_W^4)$ , is to induce a shift of  $\Delta\Gamma^{(2)} = 2\Gamma^{(0)} \Pi_{WW}^{(2)}(0) / M_W^2$  or equivalently produce a contribution of  $\Pi_{WW}^{(2)}(0) / M_W^2$  to  $\Delta r^{(2)}$ . Also listed are the divergent parts of the diagrams at general  $q^2$ . The diagrams are labeled according to Fig.2. Thus  $\Pi_{WW}^{(2a)}(0)$  denotes the contribution from diagram of Fig.2(a) at  $q^2 = 0$  and  $\Delta\Pi_{WW}^{(2a)}(q^2)$  denotes its divergent part at general  $q^2$  with  $\epsilon = 2 - n/2$ . In the following expressions, an overall common factor of  $(g^2 / (16\pi)^2)^2 \delta_{\mu\nu}$  has been omitted for brevity and

$$\tilde{B}_0(q^2, M_1^2, M_2^2) \equiv - \int_0^1 \ln(-q^2 x^2 + (q^2 - M_1^2 + M_2^2)x + M_1^2 - i\epsilon) dx.$$

### Diagram (a)

Internal photon

$$\begin{aligned}
\Pi_{WW}^{(2a)}(0) &= -10s_\theta^2 \frac{(n-2)}{n} I_0(-1, 2, 1, 1, n, M_W^2) \\
\Delta\Pi_{WW}^{(2a)}(q^2) &= \frac{s_\theta^2}{9\epsilon^2} \{45 M_W^2 - 22 q^2\} \\
&+ \frac{s_\theta^2}{54\epsilon q^4} \left\{ 240 M_W^4 q^2 + 1077 M_W^2 q^4 - 442 q^6 \right. \\
&\quad + [240 M_W^6 + 792 M_W^4 q^2 - 540 M_W^2 q^4] \ln M_W^2 \\
&\quad \left. - [240 M_W^6 + 792 M_W^4 q^2 - 264 q^6] \ln(q^2 + M_W^2) \right\}
\end{aligned} \tag{B.1}$$

Internal  $Z^0$

$$\begin{aligned}
\Pi_{WW}^{(2a)}(0) &= -10c_\theta^2 \frac{(n-2)}{n} I_2(-2, n, M_Z^2, M_W^2) \\
\Delta\Pi_{WW}^{(2a)}(q^2) &= -\frac{1}{18\epsilon^2} \{44 c_\theta^2 q^2 - 45 M_W^2 (3 - 2 s_\theta^2)\} \\
&+ \frac{1}{\epsilon (216 c_\theta^4 (1 + c_\theta^2) M_W^2 q^4 + 108 c_\theta^6 q^6 + 108 c_\theta^2 M_W^4 q^2 s_\theta^4)} \\
&\quad \times \left\{ 172 c_\theta^8 q^8 + c_\theta^6 M_W^2 q^6 (2011 + 48 \ln c_\theta^2 - 1442 s_\theta^2) \right. \\
&\quad + 12 M_W^8 s_\theta^4 (33 - 40 s_\theta^2) (\ln c_\theta^2 + s_\theta^2) \\
&\quad + 2 c_\theta^4 M_W^4 q^4 (1350 + 6 \ln c_\theta^2 - 1449 s_\theta^2 + 368 s_\theta^4) \\
&\quad + 3 c_\theta^2 M_W^6 q^2 [8 \ln c_\theta^2 (78 - 149 s_\theta^2 + 66 s_\theta^4) + s_\theta^2 (624 - 943 s_\theta^2 + 338 s_\theta^4)] \\
&\quad - [12 M_W^8 s_\theta^6 (33 - 40 s_\theta^2) + 24 c_\theta^6 M_W^2 q^6 (25 - 23 s_\theta^2) \\
&\quad + 12 c_\theta^4 M_W^4 q^4 (92 - 95 s_\theta^2 + 4 s_\theta^4) \\
&\quad + 24 M_W^6 q^2 s_\theta^2 (72 - 190 s_\theta^2 + 159 s_\theta^4 - 41 s_\theta^6)] \ln M_W^2 \\
&\quad - [528 c_\theta^8 q^8 + 12 c_\theta^6 M_W^2 q^6 (91 - 44 s_\theta^2) + 12 M_W^8 s_\theta^6 (33 - 40 s_\theta^2) \\
&\quad - 12 c_\theta^4 M_W^4 q^4 (448 - 535 s_\theta^2 + 132 s_\theta^4) \\
&\quad \left. + 12 M_W^6 q^2 s_\theta^2 (144 - 515 s_\theta^2 + 543 s_\theta^4 - 172 s_\theta^6)] \tilde{B}_0(q^2, M_W^2, M_Z^2) \right\}
\end{aligned} \tag{B.2}$$

### Diagram (b)

$$\begin{aligned}
\Pi_{WW}^{(2b)}(0) &= 2 \frac{(n-2)(n-1)}{n} I_0(-1, 2, 1, 1, n, M_W^2) \\
\Delta\Pi_{WW}^{(2b)}(q^2) &= -\frac{3 M_W^2}{\epsilon^2} - \frac{M_W^2}{2\epsilon} \{5 - 12 \ln M_W^2\}
\end{aligned} \tag{B.3}$$

**Diagram (c)**

$$\begin{aligned}
\Pi_{WW}^{(2c)}(0) &= -2M_W^2 \frac{(n-2)}{n} I_2(-1, n, M_H^2, M_W^2) \\
\Delta\Pi_{WW}^{(2c)}(q^2) &= -\frac{M_W^2}{2\epsilon^2} \\
&\quad - \frac{M_W^2}{\epsilon (24 c_h^4 (1 + c_h^2) M_W^2 q^4 + 12 c_h^6 q^6 + 12 c_h^2 M_W^4 q^2 s_h^4)} \\
&\quad \times \left\{ 5 c_h^6 q^6 - 2 c_h^4 M_W^2 q^4 (6 + 2 \ln c_h^2 - 9 s_h^2) - 4 M_W^6 s_h^4 (\ln c_h^2 + s_h^2) \right. \\
&\quad + c_h^2 M_W^4 q^2 (16 \ln c_h^2 + 16 s_h^2 - 24 s_h^2 \ln c_h^2 - 19 s_h^4) \\
&\quad + [8 c_h^2 M_W^4 q^2 s_h^4 + 4 M_W^6 s_h^6 + 4 c_h^4 M_W^2 q^4 (4 - 3 s_h^2)] \ln M_W^2 \\
&\quad + [12 c_h^6 q^6 + 20 c_h^2 M_W^4 q^2 s_h^4 + 4 M_W^6 s_h^6 \\
&\quad \left. + 4 c_h^4 M_W^2 q^4 (16 - 9 s_h^2)] \tilde{B}_0(q^2, M_H^2, M_W^2) \right\}
\end{aligned} \tag{B.4}$$

**Diagram (d)**

Internal photon

$$\begin{aligned}
\Pi_{WW}^{(2d)}(0) &= -\frac{80}{3} s_\theta^4 \frac{(n-2)}{n} I_0(0, 1, 1, 1, n, M_W^2) \\
\Delta\Pi_{WW}^{(2d)}(q^2) &= \frac{s_\theta^4}{27\epsilon^2} \{180 M_W^2 - 176 q^2\} \\
&\quad + \frac{s_\theta^4}{81\epsilon q^4} \left\{ 168 M_W^4 q^2 + 2418 M_W^2 q^4 - 1768 q^6 \right. \\
&\quad + [168 M_W^6 + 1152 M_W^4 q^2 - 1152 M_W^2 q^4] \ln M_W^2 \\
&\quad \left. - [168 M_W^6 + 1152 M_W^4 q^2 - 72 M_W^2 q^4 - 1056 q^6] \ln(q^2 + M_W^2) \right\}
\end{aligned} \tag{B.5}$$

Internal  $Z^0$

$$\begin{aligned}
\Pi_{WW}^{(2d)}(0) &= -10 \left(1 - 2s_\theta^2 + \frac{8}{3}s_\theta^4\right) \frac{(n-2)}{n} I_2(-2, n, M_W^2, M_Z^2) \quad (\text{B.6}) \\
\Delta\Pi_{WW}^{(2d)}(q^2) &= -\frac{(3 - 6s_\theta^2 + 8s_\theta^4)}{54c_\theta^2\epsilon^2} \{44c_\theta^2q^2 - 45M_W^2(3 - s_\theta^2)\} \\
&+ \frac{(3 - 6s_\theta^2 + 8s_\theta^4)}{\epsilon(648c_\theta^6(1 + c_\theta^2)M_W^2q^4 + 324c_\theta^8q^6 + 324c_\theta^4M_W^4q^2s_\theta^4)} \\
&\times \left\{ 172c_\theta^8q^8 + c_\theta^6M_W^2q^6(2011 + 552\ln c_\theta^2 - 569s_\theta^2) \right. \\
&\quad - 12M_W^8s_\theta^4(\ln c_\theta^2 + s_\theta^2)(33 + 7s_\theta^2) \\
&\quad + 2c_\theta^4M_W^4q^4(1350 - 1251s_\theta^2 + 269s_\theta^4 + 6\ln c_\theta^2(91 - 87s_\theta^2)) \\
&\quad - 3c_\theta^2M_W^6q^2(8\ln c_\theta^2(78 - 13s_\theta^2 - 24s_\theta^4) + s_\theta^2(624 - 305s_\theta^2 + 19s_\theta^4)) \\
&\quad - [24c_\theta^6M_W^2q^6(25 - 2s_\theta^2) - 12M_W^8s_\theta^6(33 + 7s_\theta^2) \\
&\quad\quad + 12c_\theta^4M_W^4q^4(92 - 89s_\theta^2 + s_\theta^4) \\
&\quad\quad - 24M_W^6q^2s_\theta^2(72 - 98s_\theta^2 + 21s_\theta^4 + 5s_\theta^6)] \ln M_W^2 \\
&\quad - [528c_\theta^8q^8 + 12c_\theta^6M_W^2q^6(91 - 47s_\theta^2) - 12M_W^8s_\theta^6(33 + 7s_\theta^2) \\
&\quad\quad - 12c_\theta^4M_W^4q^4(448 - 361s_\theta^2 + 45s_\theta^4) \\
&\quad\quad \left. - 12M_W^6q^2s_\theta^2(144 - 61s_\theta^2 - 138s_\theta^4 + 55s_\theta^6)] \tilde{B}_0(q^2, M_W^2, M_Z^2) \right\}
\end{aligned}$$

Internal  $Z$ - $\gamma$  mixing

$$\begin{aligned}
\Pi_{WW}^{(2d)}(0) &= -20s_\theta^2 \left(1 - \frac{8}{3}s_\theta^2\right) \frac{(n-2)}{n} I_1(-1, n, M_W^2, M_Z^2) \quad (\text{B.7}) \\
\Delta\Pi_{WW}^{(2d)}(q^2) &= -\frac{s_\theta^2(3 - 8s_\theta^2)}{27c_\theta^2\epsilon^2} \{44c_\theta^2q^2 - 45M_W^2(2 - s_\theta^2)\} \\
&+ \frac{s_\theta^2(3 - 8s_\theta^2)}{162c_\theta^4\epsilon M_W^2q^4} \left\{ 240c_\theta^6q^8 + 4c_\theta^4M_W^2q^6(67 - 30\ln c_\theta^2 - 114s_\theta^2) \right. \\
&\quad - 12M_W^6q^2(1 - (3 - 11\ln c_\theta^2)s_\theta^2 + (14 - \ln c_\theta^2)s_\theta^4 - 2s_\theta^6) \\
&\quad + 3c_\theta^2M_W^4q^4(300 - 255s_\theta^2 + 64s_\theta^4 + 4\ln c_\theta^2(2 + 9s_\theta^2)) \\
&\quad - [12c_\theta^6M_W^8 - 120c_\theta^4M_W^2q^6(2 - s_\theta^2) \\
&\quad\quad - 12M_W^6q^2(7 - 21s_\theta^2 + 32s_\theta^4 - 8s_\theta^6) \\
&\quad\quad + 12M_W^4q^4(7 + 16s_\theta^2 - 42s_\theta^4 + 19s_\theta^6)] \ln M_W^2 \\
&\quad + [12c_\theta^6M_W^8 - 84c_\theta^6M_W^6q^2 - 324c_\theta^6M_W^4q^4 - 348c_\theta^6M_W^2q^6 \\
&\quad\quad - 120c_\theta^6q^8] \ln(q^2 + M_W^2) \\
&\quad - [120c_\theta^6q^8 + 12c_\theta^4M_W^2q^6(53 - 19s_\theta^2) - 12M_W^6q^2s_\theta^4(11 - s_\theta^2) \\
&\quad\quad \left. - 24M_W^4q^4(28 - 35s_\theta^2 + 3s_\theta^4 + 4s_\theta^6)] \tilde{B}_0(q^2, M_W^2, M_Z^2) \right\}
\end{aligned}$$

### Diagram (e)

Internal photon

$$\Pi_{WW}^{(2e)}(0) = 0 \quad (\text{B.8})$$

$$\Delta\Pi_{WW}^{(2e)}(q^2) = 0 \quad (\text{B.9})$$

Internal  $Z^0$

$$\Pi_{WW}^{(2e)}(0) = 2 \left( 1 - 2s_\theta^2 + \frac{8}{3}s_\theta^4 \right) \frac{(n-1)(n-2)}{n} I_0(-1, 2, 1, 1, n, M_Z^2) \quad (\text{B.10})$$

$$\begin{aligned} \Delta\Pi_{WW}^{(2e)}(q^2) = & -\frac{M_W^2 (3 - 6s_\theta^2 + 8s_\theta^4)}{c_\theta^2 \epsilon^2} \\ & - \frac{M_W^2 (3 - 6s_\theta^2 + 8s_\theta^4)}{6c_\theta^2 \epsilon} \{5 + 12 \ln c_\theta^2 - 12 \ln M_W^2\} \end{aligned}$$

Internal  $Z$ - $\gamma$  mixing

$$\Pi_{WW}^{(2e)}(0) = 4s_\theta^2 \left( 1 - \frac{8}{3}s_\theta^2 \right) \frac{(n-1)(n-2)}{n} I_0(0, 1, 1, 1, n, M_Z^2) \quad (\text{B.11})$$

$$\begin{aligned} \Delta\Pi_{WW}^{(2e)}(q^2) = & -\frac{M_W^2 s_\theta^2 (3 - 8s_\theta^2)}{c_\theta^2 \epsilon^2} \\ & - \frac{M_W^2 s_\theta^2 (3 - 8s_\theta^2)}{6c_\theta^2 \epsilon} \{11 + 12 \ln c_\theta^2 - 12 \ln M_W^2\} \end{aligned}$$

### Diagram (f)

Internal photon

$$\Pi_{WW}^{(2f)}(0) = -M_W^2 \frac{16}{3} s_\theta^4 \frac{(n-2)}{n} I_0(1, 1, 1, 1, n, M_W^2) \quad (\text{B.12})$$

$$\begin{aligned} \Delta\Pi_{WW}^{(2f)}(q^2) = & -\frac{4M_W^2 s_\theta^4}{3\epsilon^2} \\ & - \frac{M_W^2 s_\theta^4}{9\epsilon q^4} \left\{ 8M_W^2 q^2 + 58q^4 + [8M_W^4 + 32M_W^2 q^2] \ln M_W^2 \right. \\ & \left. - [8M_W^4 + 32M_W^2 q^2 + 24q^4] \ln(q^2 + M_W^2) \right\} \end{aligned}$$

Internal  $Z^0$

$$\begin{aligned}
\Pi_{WW}^{(2f)}(0) &= -2M_W^2 \frac{s_\theta^4}{c_\theta^4} \left(1 - 2s_\theta^2 + \frac{8}{3}s_\theta^4\right) \frac{(n-2)}{n} I_2(-1, n, M_W^2, M_Z^2) \quad (\text{B.13}) \\
\Delta\Pi_{WW}^{(2f)}(q^2) &= -\frac{M_W^2 s_\theta^4 (3 - 6s_\theta^2 + 8s_\theta^4)}{6c_\theta^4 \epsilon^2} \\
&+ \frac{M_W^2 s_\theta^4 (3 - 6s_\theta^2 + 8s_\theta^4)}{\epsilon (72c_\theta^8 (1 + c_\theta^2) M_W^2 q^4 + 36c_\theta^{10} q^6 + 36c_\theta^6 M_W^4 q^2 s_\theta^4)} \\
&\times \left\{ -5c_\theta^6 q^6 - 4M_W^6 s_\theta^4 (\ln c_\theta^2 + s_\theta^2) + 6c_\theta^4 M_W^2 q^4 (2 + 2\ln c_\theta^2 + s_\theta^2) \right. \\
&\quad + c_\theta^2 M_W^4 q^2 (8\ln c_\theta^2 (2 - s_\theta^2) + s_\theta^2 (16 + 3s_\theta^2)) \\
&\quad - [8c_\theta^2 M_W^4 q^2 s_\theta^4 - 4M_W^6 s_\theta^6 + 4c_\theta^4 M_W^2 q^4 (4 - s_\theta^2)] \ln M_W^2 \\
&\quad \left. - [12c_\theta^6 q^6 + 20c_\theta^2 M_W^4 q^2 s_\theta^4 - 4M_W^6 s_\theta^6 \right. \\
&\quad \left. + 4c_\theta^4 M_W^2 q^4 (16 - 7s_\theta^2)] \tilde{B}_0(q^2, M_W^2, M_Z^2) \right\}
\end{aligned}$$

Internal  $Z$ - $\gamma$  mixing

$$\begin{aligned}
\Pi_{WW}^{(2f)}(0) &= 4\frac{s_\theta^4}{c_\theta^2} \left(1 - \frac{8}{3}s_\theta^2\right) \frac{(n-2)}{n} I_1(0, n, M_W^2, M_Z^2) \quad (\text{B.14}) \\
\Delta\Pi_{WW}^{(2f)}(q^2) &= \frac{M_W^2 s_\theta^4 (3 - 8s_\theta^2)}{3c_\theta^2 \epsilon^2} \\
&+ \frac{s_\theta^2 (3 - 8s_\theta^2)}{54c_\theta^6 \epsilon q^4} \left\{ 8c_\theta^6 q^6 s_\theta^2 + c_\theta^4 M_W^2 q^4 s_\theta^2 (19 - 4\ln c_\theta^2 - 16s_\theta^2) \right. \\
&\quad + 4c_\theta^2 M_W^4 q^2 s_\theta^2 (1 - (2 - \ln c_\theta^2) s_\theta^2 + 2s_\theta^4) \\
&\quad + [4c_\theta^6 M_W^6 s_\theta^2 + 4c_\theta^4 M_W^2 q^4 s_\theta^2 (2 - s_\theta^2) \\
&\quad \quad + 4M_W^4 q^2 s_\theta^2 (3 - 9s_\theta^2 + 8s_\theta^4 - 2s_\theta^6)] \ln M_W^2 \\
&\quad - [4c_\theta^6 M_W^6 s_\theta^2 + 12c_\theta^6 M_W^4 q^2 s_\theta^2 + 12c_\theta^6 M_W^2 q^4 s_\theta^2 + 4c_\theta^6 q^6 s_\theta^2] \ln(q^2 + M_W^2) \\
&\quad \left. - [4c_\theta^6 q^6 s_\theta^2 + 4c_\theta^2 M_W^4 q^2 s_\theta^6 - 8c_\theta^4 M_W^2 q^4 s_\theta^2 (4 + s_\theta^2)] \tilde{B}_0(q^2, M_W^2, M_Z^2) \right\}
\end{aligned}$$

**Diagrams (g), (h), (i) and (j)**

Internal photon

$$\begin{aligned} \Pi_{WW}^{(2g+h+i+j)}(0) = & 8s_\theta^2 \frac{(n-2)}{n} \{2I_0(0, 1, 1, 1, n, M_W^2) - I_0(1, 1, 2, -1, n, M_W^2) \\ & - I_0(-1, 1, 2, 1, n, M_W^2)\} \end{aligned} \quad (\text{B.15})$$

$$\begin{aligned} \Delta\Pi_{WW}^{(2g+h+i+j)}(q^2) = & -\frac{s_\theta^2}{9\epsilon^2} \{54 M_W^2 - 2q^2\} \\ & - \frac{s_\theta^2}{27\epsilon q^4} \left\{ 60 M_W^4 q^2 + 519 M_W^2 q^4 + 59 q^6 \right. \\ & + [60 M_W^6 + 252 M_W^4 q^2 - 360 M_W^2 q^4] \ln M_W^2 - 216 q^6 \ln q^2 \\ & \left. - [60 M_W^6 + 252 M_W^4 q^2 - 36 M_W^2 q^4 - 228 q^6] \ln(q^2 + M_W^2) \right\} \end{aligned}$$

Internal  $Z^0$

$$\begin{aligned} \Pi_{WW}^{(2g+h+i+j)}(0) = & \frac{8c_\theta^4}{M_W^2 s_\theta^2} \frac{(n-2)}{n} \{I_0(0, 1, 2, -1, n, M_Z^2) - I_0(0, 1, 2, -1, n, M_W^2) \\ & + I_0(-2, 1, 2, 1, n, M_Z^2) - I_0(-2, 1, 2, 1, n, M_W^2) \\ & - 2I_0(-1, 1, 1, 1, n, M_Z^2) + 2I_0(-1, 1, 1, 1, n, M_W^2)\} \end{aligned} \quad (\text{B.16})$$

$$\begin{aligned} \Delta\Pi_{WW}^{(2g+h+i+j)}(q^2) = & \frac{1}{9\epsilon^2} \{q^2 (2 - 2s_\theta^2) - 54 M_W^2 (2 - s_\theta^2)\} \\ & - \frac{1}{27 c_\theta^2 \epsilon q^2} \left\{ 515 c_\theta^4 q^4 - 60 M_W^4 s_\theta^2 (\ln c_\theta^2 + s_\theta^2) + 3 c_\theta^2 M_W^2 q^2 (44 \ln c_\theta^2 + 45 (2 - s_\theta^2)) \right. \\ & + [60 M_W^4 s_\theta^4 - 132 M_W^2 q^2 (2 - 3s_\theta^2 + s_\theta^4)] \ln M_W^2 - 216 c_\theta^4 q^4 \ln q^2 \\ & \left. - [228 c_\theta^4 q^4 - 60 M_W^4 s_\theta^4 - 192 M_W^2 q^2 (2 - 3s_\theta^2 + s_\theta^4)] \tilde{B}_0(q^2, M_W^2, M_Z^2) \right\} \end{aligned}$$

**Diagrams (k) and (l)**

$$\Pi_{WW}^{(2k+l)}(0) = 2 \frac{(n-2)^2}{n} \{I_0(-1, 1, 2, 1, n, M_W^2) - I_0(0, 1, 1, 1, n, M_W^2)\} \quad (\text{B.17})$$

$$\Delta\Pi_{WW}^{(2k+l)}(q^2) = \frac{1}{3\epsilon^2} \{6 M_W^2 + 2q^2\} + \frac{1}{\epsilon} \left\{ M_W^2 + \frac{8q^2}{3} - 4 M_W^2 \ln M_W^2 - \frac{4q^2 \ln q^2}{3} \right\}$$

**Diagram (m)**

Internal photon

$$\begin{aligned} \Pi_{WW}^{(2m)}(0) = & 0 \\ \Delta\Pi_{WW}^{(2m)}(q^2) = & \frac{2q^2 s_\theta^2}{9\epsilon^2} + \frac{q^2 s_\theta^2}{9\epsilon} \{11 - 4 \ln q^2\} \end{aligned} \quad (\text{B.18})$$

Internal  $Z^0$

$$\begin{aligned} \Pi_{WW}^{(2m)}(0) = & -\frac{1}{c_\theta^2} \left( 1 - 2s_\theta^2 + \frac{2}{3}s_\theta^4 \right) \frac{(n-2)}{n} \{ (n-2)I_0(0, 1, 1, 1, n, M_Z^2) \\ & - 4I_0(-1, 1, 2, 1, n, M_Z^2) \\ & + I_0(-2, 1, 2, 2, n, M_Z^2) \} \end{aligned} \quad (\text{B.19})$$

$$\begin{aligned} \Delta\Pi_{WW}^{(2m)}(q^2) = & \frac{(3 - 6s_\theta^2 + 2s_\theta^4)}{9c_\theta^4\epsilon^2} \{ 3M_W^2 + c_\theta^2 q^2 \} \\ & + \frac{(3 - 6s_\theta^2 + 2s_\theta^4)}{18c_\theta^4\epsilon} \left\{ 3(1 + 4\ln c_\theta^2) M_W^2 + 11c_\theta^2 q^2 - 12M_W^2 \ln M_W^2 - 4c_\theta^2 q^2 \ln q^2 \right\} \end{aligned}$$

### Diagrams (n) and (o)

Internal photon

$$\begin{aligned} \Pi_{WW}^{(2n+o)}(0) = & 0 \\ \Delta\Pi_{WW}^{(2n+o)}(q^2) = & \frac{4q^2 s_\theta^2}{9\epsilon^2} + \frac{q^2 s_\theta^2}{9\epsilon} \{ 16 - 8\ln q^2 \} \end{aligned} \quad (\text{B.20})$$

Internal  $Z^0$

$$\begin{aligned} \Pi_{WW}^{(2n+o)}(0) = & \frac{1}{c_\theta^2} \left( 1 - 2s_\theta^2 + \frac{4}{3}s_\theta^4 \right) \frac{(n-2)^2}{n} \{ I_0(-1, 1, 2, 1, n, M_Z^2) \\ & - I_0(0, 1, 1, 1, n, M_Z^2) \} \end{aligned} \quad (\text{B.21})$$

$$\begin{aligned} \Delta\Pi_{WW}^{(2n+o)}(q^2) = & \frac{(3 - 6s_\theta^2 + 4s_\theta^4)}{9c_\theta^4\epsilon^2} \{ 3M_W^2 + c_\theta^2 q^2 \} \\ & + \frac{(3 - 6s_\theta^2 + 4s_\theta^4)}{18c_\theta^4\epsilon} \left\{ 3(1 + 4\ln c_\theta^2) M_W^2 + 8c_\theta^2 q^2 - 12M_W^2 \ln M_W^2 - 4c_\theta^2 q^2 \ln q^2 \right\} \end{aligned} \quad (\text{B.22})$$

### Tadpole Diagrams

For completeness the contributions of the  $\mathcal{O}(N_f\alpha^2)$  tadpole diagrams, Fig.1, are given. As above an overall factor of  $(g^2/(16\pi)^2)^2 \delta_{\mu\nu}$  has been omitted from all diagrams.

#### Diagram (a)

$$\Pi_{WW}^{(2a)}(0) = -2c_h^2(n-2)I_0(-1, 2, 1, 1, n, M_W^2) \quad (\text{B.23})$$

#### Diagram (b)

$$\Pi_{WW}^{(2b)}(0) = -2\frac{M_W^2}{c_h^2 c_\theta^2} \left( 1 - 2s_\theta^2 + \frac{8}{3}s_\theta^4 \right) (n-2)I_0(-1, 2, 1, 1, n, M_W^2) \quad (\text{B.24})$$



## C Vertex Corrections

In this appendix the vertex and external leg corrections for massless on-shell fermions coupling to the  $W$  boson are given. These take general form

$$i\frac{g}{\sqrt{2}}\gamma_\mu\gamma_L V^{(2)}(0)$$

with the contribution of the various diagrams to  $V^{(2)}(0)$  being given below. Their net effect on the inverse muon lifetime is to induce a shift of  $\Delta\Gamma^{(2)} = 4\Gamma^{(0)}V^{(2)}(0)$  or equivalently produce a contribution of  $2V^{(2)}(0)$  to  $\Delta r^{(2)}$ .

The diagrams are labeled according to Fig.3. An overall factor of  $(g^2/(16\pi)^2)^2$  has been omitted from all diagrams.

### Diagrams (a), (b) and (c)

Internal photon

$$V^{(2a+b+c)}(0) = \frac{8}{3}s_\theta^4 \frac{(n-2)(n-4)}{n} I_0(1, 1, 1, 1, n, \Lambda^2) \quad (\text{C.1})$$

Internal  $Z^0$

$$V^{(2a+b+c)}(0) = \left(1 - 2s_\theta^2 + \frac{8}{3}s_\theta^4\right) \frac{(n-2)(n-4)}{n} I_0(0, 2, 1, 1, n, M_Z^2) \quad (\text{C.2})$$

Internal  $Z$ - $\gamma$  mixing

$$V^{(2a+b+c)}(0) = 2s_\theta^2 \left(1 - \frac{8}{3}s_\theta^2\right) \frac{(n-2)(n-4)}{n} I_0(1, 1, 1, 1, n, M_Z^2) \quad (\text{C.3})$$

### Diagrams (d) and (e)

$$V^{(2d+e)}(0) = \frac{(n-2)(n-4)}{n} I_0(0, 2, 1, 1, n, M_W^2) \quad (\text{C.4})$$

### Diagrams (f) and (g)

Internal photon

$$V^{(2f+g)}(0) = -16s_\theta^4 \frac{(n-2)}{n} I_0(1, 1, 1, 1, n, M_W^2) \quad (\text{C.5})$$

Internal  $Z^0$

$$V^{(2f+g)}(0) = -6 \left( 1 - 2s_\theta^2 + \frac{8}{3}s_\theta^4 \right) \frac{(n-2)}{n} I_2(-1, n, M_W^2, M_Z^2) \quad (\text{C.6})$$

Internal  $Z$ - $\gamma$  mixing

$$V^{(2f+g)}(0) = -12 \left( 1 - \frac{8}{3}s_\theta^2 \right) \frac{(n-2)}{n} I_1(0, n, M_W^2, M_Z^2) \quad (\text{C.7})$$

**Diagrams (h) and (i)**

Internal photon

$$V^{(2h+i)}(0) = -6s_\theta^2 \frac{(n-2)}{n} I_0(0, 2, 1, 1, n, M_W^2) \quad (\text{C.8})$$

Internal  $Z^0$

$$V^{(2h+i)}(0) = -6c_\theta^2 \frac{(n-2)}{n} I_2(-1, n, M_Z^2, M_W^2) \quad (\text{C.9})$$

**Diagrams (j), (k), (l) and (m)**

Internal photon

$$V^{(2j+k+l+m)}(0) = 2s_\theta^2 \frac{(n-2)}{n} \{ 3I_0(1, 1, 1, 1, n, M_W^2) - I_0(2, 1, 2, -1, n, M_W^2) \\ - I_0(0, 1, 2, 1, n, M_W^2) \} \quad (\text{C.10})$$

Internal  $Z^0$

$$V^{(2j+k+l+m)}(0) = \frac{2c_\theta^4}{M_W^2 s_\theta^2} \frac{(n-2)}{n} \{ 3I_0(0, 1, 1, 1, n, M_W^2) - 3I_0(0, 1, 1, 1, n, M_Z^2) \\ - I_0(1, 1, 2, -1, n, M_W^2) + I_0(1, 1, 2, -1, n, M_Z^2) \\ - I_0(-1, 1, 2, 1, n, M_W^2) + I_0(-1, 1, 2, 1, n, M_Z^2) \} \quad (\text{C.11})$$

## D Box Diagrams

In this appendix expressions are given for the box diagrams of Fig.4. The methods used in their calculation have been discussed in section 4.3. All diagrams are simply

proportional to the tree-level muon decay amplitude. Their net effect on the inverse muon lifetime is to induce a shift of  $\Delta\Gamma^{(2)} = 2\Gamma^{(0)}B^{(2)}$  or equivalently produce a contribution of  $B$  to  $\Delta r^{(2)}$ . The diagrams are labeled according to Fig.4 An overall factor of  $(g^2/(16\pi)^2)^2$  has been omitted from all diagrams.

### Diagrams (a) and (b)

Internal  $Z^0$

$$B^{(2a+b)} = -\frac{2}{c_\theta^4}(1-2s_\theta^2)\left(1-2s_\theta^2+\frac{8}{3}s_\theta^4\right)\frac{(n-2)}{n}I_1(0,n,M_W^2,M_Z^2) \quad (\text{D.1})$$

Internal  $Z$ - $\gamma$  mixing

$$B^{(2a+b)}(0) = -4\frac{s_\theta^2}{c_\theta^2}\left(1-\frac{8}{3}s_\theta^2\right)\frac{(n-2)}{n}I_1(1,n,M_W^2,M_Z^2) \quad (\text{D.2})$$

### Diagrams (c) and (d)

$$B^{(2c+d)} = -\frac{2}{c_\theta^2}(1-2s_\theta^2)\frac{(n-2)}{n}I_2(0,n,M_Z^2,M_W^2) \quad (\text{D.3})$$

## E Counterterm Insertions

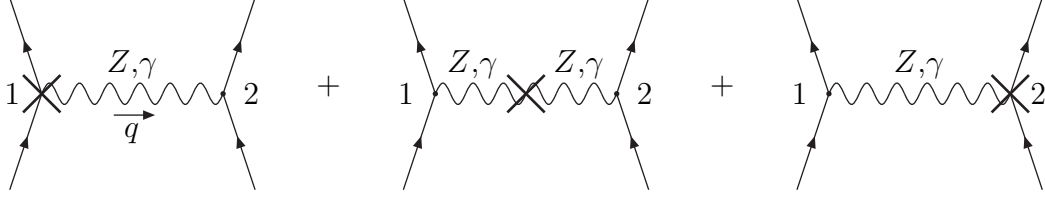
For an internal line in a Feynman diagram, representing a physical particle, there is a cancellation of wavefunction counterterms between those in the 2-point counterterm and those in vertices at its endpoints. While this happens trivially for the  $W$  boson, the cancellation is less straightforward in the case of neutral bosons where  $Z$ - $\gamma$  mixing is a complicating factor.

In this appendix, identities, valid to  $\mathcal{O}(\alpha)$ , are given for the counterterm insertions on internal neutral boson lines. The cancellation of the wavefunction counterterms,  $\delta Z_W^{(1)}$  and  $\delta Z_B^{(1)}$ , has been explicitly carried out. Note that wavefunction counterterms associated with the external particles have not been included and must be taken into account separately. A similar cancellation of wavefunction counterterms in the presence of  $Z$ - $\gamma$  mixing was carried out in ref. [28].

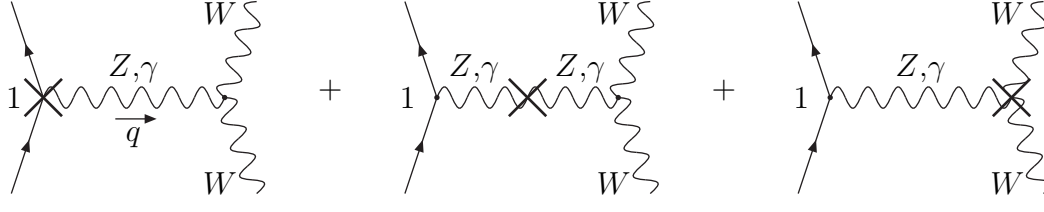
As in the text the notation  $Z,\gamma$  means that all possibilities are to be included. In the identities,  $g\beta_L$  and  $g\beta_R$  are the left- and right-handed couplings of the  $Z^0$  to the fermion

$$\beta_L = \frac{t_3 - s_\theta^2 Q}{c_\theta}, \quad \beta_R = -\frac{s_\theta^2 Q}{c_\theta} \quad (\text{E.1})$$

in which  $t_3$  is its weak isospin and  $Q$  is its electric charge. Unprimed quantities are associated with the fermion current labeled 1 and primed with the current labeled 2. Square brackets  $[ ]$  indicate that the enclosed quantities pertain to the fermion current given by the its subscript



$$\begin{aligned}
&= \frac{2}{q^2} \left( s_\theta^2 \frac{\delta g^{(1)}}{g} + c_\theta^2 \frac{\delta g'^{(1)}}{g'} \right) [igs_\theta Q \gamma_\mu]_1 [igs_\theta Q' \gamma_\mu]_2 \\
&+ \frac{2s_\theta c_\theta}{q^2 + M_Z^2} \left( \frac{\delta g^{(1)}}{g} - \frac{\delta g'^{(1)}}{g'} \right) [igs_\theta Q \gamma_\mu]_1 [ig\gamma_\mu(\beta'_L \gamma_L + \beta'_R \gamma_R)]_2 \\
&+ \frac{2s_\theta c_\theta}{q^2 + M_Z^2} \left( \frac{\delta g^{(1)}}{g} - \frac{\delta g'^{(1)}}{g'} \right) [ig\gamma_\mu(\beta_L \gamma_L + \beta_R \gamma_R)]_1 [igs_\theta Q' \gamma_\mu]_2 \\
&+ \frac{2}{q^2 + M_Z^2} \left( c_\theta^2 \frac{\delta g^{(1)}}{g} + s_\theta^2 \frac{\delta g'^{(1)}}{g'} \right) [ig\gamma_\mu(\beta_L \gamma_L + \beta_R \gamma_R)]_1 [ig\gamma_\mu(\beta'_L \gamma_L + \beta'_R \gamma_R)]_2 \\
&- \frac{\delta M_Z^{2(1)}}{(q^2 + M_Z^2)^2} [ig\gamma_\mu(\beta_L \gamma_L + \beta_R \gamma_R)]_1 [ig\gamma_\mu(\beta'_L \gamma_L + \beta'_R \gamma_R)]_2
\end{aligned} \tag{E.2}$$



$$\begin{aligned}
&= \frac{2}{q^2} \left( s_\theta^2 \frac{\delta g^{(1)}}{g} + c_\theta^2 \frac{\delta g'^{(1)}}{g'} \right) [igs_\theta Q \gamma_\mu]_1 (gs_\theta) \\
&+ \frac{2s_\theta c_\theta}{q^2 + M_Z^2} \left( \frac{\delta g^{(1)}}{g} - \frac{\delta g'^{(1)}}{g'} \right) [igs_\theta Q \gamma_\mu]_1 (gc_\theta) \\
&+ \frac{2}{q^2 + M_Z^2} \left( \frac{\delta g^{(1)}}{g} \right) [ig\gamma_\mu(\beta_L \gamma_L + \beta_R \gamma_R)]_1 (gc_\theta) \\
&- \frac{\delta M_Z^{2(1)}}{(q^2 + M_Z^2)^2} [ig\gamma_\mu(\beta_L \gamma_L + \beta_R \gamma_R)]_1 (gc_\theta)
\end{aligned} \tag{E.3}$$

$$\begin{aligned}
&= \frac{2}{q^2} \left( s_\theta^2 \frac{\delta g^{(1)}}{g} + c_\theta^2 \frac{\delta g'^{(1)}}{g'} \right) (gs_\theta) (gs_\theta) \\
&+ \frac{2s_\theta c_\theta}{q^2 + M_Z^2} \left( \frac{\delta g^{(1)}}{g} - \frac{\delta g'^{(1)}}{g'} \right) (gs_\theta) (gc_\theta) \\
&+ \frac{2}{q^2 + M_Z^2} \left( \frac{\delta g^{(1)}}{g} \right) (gc_\theta) (gc_\theta) \\
&- \frac{\delta M_Z^2{}^{(1)}}{(q^2 + M_Z^2)^2} (gc_\theta) (gc_\theta)
\end{aligned} \tag{E.4}$$

## References

- [1] T. Kinoshita and A. Sirlin, *Phys. Rev.* **113** (1959) 1652.
- [2] T. van Ritbergen and R. G. Stuart, *Phys. Lett.* **B 437** (1998) 201.
- [3] T. van Ritbergen and R. G. Stuart, *Phys. Rev. Lett.* **82** (1999) 488.
- [4] T. van Ritbergen and R. G. Stuart, *in preparation*.
- [5] A. Sirlin, *Phys. Rev.* **D 22** (1980) 971.
- [6] D. A. Ross and M. Veltman, *Nucl. Phys.* **B 95** (1977) 135.
- [7] CDF collaboration, *Phys. Rev.* **D 50** (1994) 2966.
- [8] J. J. van der Bij and M. Veltman, *Nucl. Phys.* **B 231** (1984) 205.
- [9] J. J. van der Bij and F. Hoogeveen, *Nucl. Phys.* **B 283** (1987) 477.
- [10] M. Consoli, W. Hollik and F. Jegerlehner, *Phys. Lett.* **B 227** (1989) 167.
- [11] R. Barbieri *et al.*, *Phys. Lett.* **B 288** (1992) 95; errata *ibid* **B 312** (1993) 511.
- [12] R. Barbieri *et al.*, *Nucl. Phys.* **B 409** (1993) 105.
- [13] J. Fleischer, O. V. Tarasov and F. Jegerlehner, *Phys. Lett.* **B 319** (1993) 249.
- [14] J. Fleischer, O. V. Tarasov and F. Jegerlehner, *Phys. Rev.* **D 51** (1995) 3820.

- [15] G. Degrossi, S. Fanchiotti and P. Gambino, *Int. J. Mod. Phys. A* **10** (1995) 1337.
- [16] S. Bauberger and G. Weiglein, *Phys. Lett.* **B 419** (1998) 333.
- [17] G. Weiglein, R. Scharf and M. Böhm, *Nucl. Phys.* **B 416** (1994) 606.
- [18] P. Malde and R. G. Stuart, hep-ph/9805364.
- [19] P. Malde, Ph.D. Thesis, University of Michigan, (1999).
- [20] R. Akhoury, P. Malde and R. G. Stuart, hep-ph/9707520.
- [21] D. A. Ross and J. C. Taylor, *Nucl. Phys.* **B 51** (1973) 125.
- [22] M. Böhm, W. Hollik and H. Spiesberger, *Fortschr. Phys.* **34** (1986) 687.
- [23] W. F. L. Hollik, *Fortschr. Phys.* **38** (1990) 165.
- [24] R. Scharf and J. B. Tausk, *Nucl. Phys.* **B 412** (1994) 523.
- [25] A. Sirlin, *Rev. Mod. Phys.* **50** (1978) 573.
- [26] A. Sirlin, *Phys. Rev.* **D 29** (1984) 89.
- [27] A. Sirlin, *Nucl. Phys.* **B 192** (1981) 93.
- [28] R. G. Stuart, *Phys. Lett.* **B 272** (1991) 353.
- [29] B. A. Kniehl and R. G. Stuart, *Comput. Phys. Comm.* **72** (1992) 175.